Compressive-Sensing-Based Multiuser Detector for the Large-Scale SM-MIMO Uplink

Zhen Gao, Linglong Dai, Zhaocheng Wang, *Senior Member, IEEE*, Sheng Chen, *Fellow, IEEE*, and Lajos Hanzo, *Fellow, IEEE*

Abstract—Conventional spatial modulation (SM) is typically considered for transmission in the downlink of small-scale multiple-input–multiple-output (MIMO) systems, where a single antenna element (AE) of a set of, e.g., 2^P AEs is activated for implicitly conveying p bits. By contrast, inspired by the compelling benefits of large-scale MIMO (LS-MIMO) systems, here, we propose an LS-SM-MIMO scheme for the uplink (UL), where each user having multiple AEs but only a single radio frequency (RF) chain invokes SM for increasing the UL throughput. At the same time, by relying on hundreds of AEs and a small number of RF chains, the base station (BS) can simultaneously serve multiple users while reducing the power consumption. Due to the large number of AEs of the UL users and the comparably small number of RF chains at the BS, the UL multiuser signal detection becomes a challenging large-scale underdetermined problem. To solve this problem, we propose a joint SM transmission scheme and a carefully designed structured compressive sensing (SCS)-based multiuser detector (MUD) to be used at the users and the BS, respectively. Additionally, the cyclic-prefix single carrier (CPSC) is used to combat the multipath channels, and a simple receive AE selection is used for the improved performance over correlated Rayleigh-fading MIMO channels. We demonstrate that the aggregate SM signal consisting of multiple UL users' SM signals of a CPSC block exhibits distributed sparsity. Moreover, due to the joint SM transmission scheme, aggregate SM signals in the same transmission group exhibit group sparsity. By exploiting these intrinsically sparse features, the proposed SCS-based MUD can reliably detect the resultant SM signals with low complexity. Simulation results demonstrate that the proposed SCS-based MUD achieves a better signal detection performance than its counterparts even with higher UL throughput.

Index Terms—Compressive sensing (CS), large-scale multiple-input–multiple-output (LS-MIMO), multiuser detector (MUD), spatial modulation (SM).

I. INTRODUCTION

A widely recognized consensus is that fifth-generation (5G) systems will be capable of providing significant energy efficiency and system capacity improvements [1], [2]. Promising techniques, such as large-scale multiple-input–multiple-output (LS-MIMO) and spatial modulation (SM)-MIMO systems, are considered as potent candidates for 5G systems [1]–[5]. LS-MIMO employing hundreds of antenna elements (AEs) at the base station (BS) is capable of improving spectral efficiency by orders of magnitude, but it suffers from the

nonnegligible power consumption and hardware cost due to one specific radio frequency (RF) chain usually required by every AE [5]. By using a reduced number of RF chains, the emerging SM-MIMO activates part of available AEs to transmit extra information in the spatial domain, and it has attracted much attention due to its high energy efficiency and reduced hardware cost [5]. However, conventional SM-MIMO is usually considered in the downlink of small-scale MIMO systems, and therefore, its achievable capacity is limited. Individually, both technologies have their own advantages and drawbacks. By an effective combination of them, one can envision the win–win situation. SM-MIMO is attractive for LS-MIMO systems, since the reduced number of required RF chains in SM-MIMO can reduce the power consumption and hardware cost in conventional LS-MIMO systems. Moveover, hundreds of AEs used in LS-MIMO can improve the system throughput of SM-MIMO. Such reciprocity enables LS-MIMO and SM-MIMO to enjoy the apparent compatibility.

In this paper, we propose an LS-SM-MIMO scheme for intrinsically amalgamating the compelling benefits of both LS-MIMO and SM-MIMO for the 5G uplink (UL) over frequency-selective fading channels. In the proposed scheme, each UL user equipped with multiple AEs but only a single RF chain invokes SM for increasing the UL throughput, and the cyclic-prefix single-carrier (CPSC) transmission scheme is adopted to combat the multipath channels [6]. At the BS, hundreds of AEs but only dozens of RF chains are employed to simultaneously serve multiple users, and a direct AE selection scheme is used to improve the system performance over correlated Rayleigh-fading MIMO channels at the BS [7]. The proposed scheme can be adopted in conventional LS-MIMO as a specific UL-transmission mode for reducing the power consumption or, alternatively, for energy- and cost-efficient LS-SM-MIMO, where joint benefits of efficient AE selection [7], transmit precoding [8], and channel estimation [9] can be readily exploited. To sum up, the proposed scheme inherits the advantages of LS-MIMO and SM-MIMO, while reducing the power consumption and hardware cost.

A challenging problem in the proposed UL LS-SM-MIMO scheme is how to realize a reliable multiuser detector (MUD) with low complexity. The optimal maximum likelihood (ML) signal detector suffers from excessive complexity. Conventional sphere decoding detectors cannot be readily used in multiuser scenarios and may still exhibit high complexity for LS-SM-MIMO [10]. Existing low-complexity linear signal detectors, e.g., the minimum mean square error (MMSE)-based signal detector, perform well for conventional LS-MIMO systems [4]. However, they are unsuitable for the proposed LS-SM-MIMO UL transmission, since the large number of transmit AEs of the UL users and the reduced number of receive RF chains at the BS make UL multiuser signal detection a large-scale underdetermined/rank-deficient problem. The authors in [11]–[13] proposed compressive sensing (CS)-based signal detectors to solve the underdetermined signal detection problem in SM-MIMO systems, but they only considered the single-user small-scale SM-MIMO systems in the downlink.

Against this background, our new contribution is that we exploit the specific signal structure in the proposed multiuser LS-SM-MIMO UL transmission, where each user only activates a single AE in each time slot. Hence, the SM signal of each UL user is sparse with the sparsity level of one, and the aggregate SM signal consisting of multiple UL users' SM signals of a CPSC block exhibits certain distributed sparsity, which can be beneficially exploited for improving the signal detection performance at the BS. Moreover, we propose a joint SM transmission scheme for the UL users in conjunction with an appropriately structured CS (SCS)-based MUD at the BS. The proposed SCS-based MUD is specifically tailored to leverage
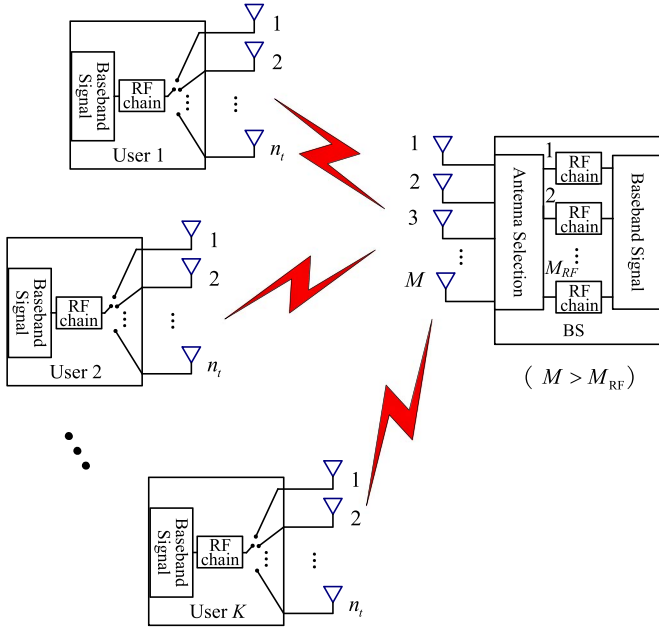
Fig. 1. In the proposed UL LS-SM-MIMO, the BS is equipped with M AEs and M_{RF} RF chains to simultaneously serve K users, where $M \gg M_{\mathrm{RF}} > K$, and each user is equipped with $n_t > 1$ AEs and one RF chain. By exploiting the improved degree of freedom in the spatial domain, multiple users can simultaneously exploit SM for improving the UL throughput.

the inherently distributed sparsity of the aggregate SM signal and the group sparsity of multiple aggregate SM signals, owing to the joint SM transmission scheme for reliable signal detection performance. Our simulation results demonstrate that the proposed SCS-based MUD is capable of outperforming the conventional detectors even with higher UL throughput.

The rest of this paper is organized as follows. Section II introduces the system model of the proposed LS-SM-MIMO scheme. Section III specifies the proposed joint SM transmission and SCS-based MUD. Section IV provides our simulation results. Section V concludes this paper.

Throughout this paper, lowercase and uppercase boldface letters denote vectors and matrices, respectively, whereas $(\cdot)^T$, $(\cdot)^*$, $(\cdot)^\dagger$, and $\lfloor \cdot \rfloor$ denote the transpose, conjugate transpose, Moore–Penrose matrix inversion, and the integer floor operators, respectively. The l_0 and l_2 norm operations are given by $\|\cdot\|_0$ and $\|\cdot\|_2$, respectively. The support set of vector $\mathbf{x}$ is denoted by $\mathrm{supp}\{\mathbf{x}\}$, and $\mathbf{x}\rangle_i$ denotes the ith entry of vector $\mathbf{x}$. Additionally, $\mathbf{x}|_\Gamma$ denotes the entries of $\mathbf{x}$ defined in the set Γ, $\mathbf{\Phi}|_\Gamma$ denotes the submatrix whose columns comprise the columns of $\mathbf{\Phi}$ that are defined in Γ, and $\mathbf{\Phi}\rangle_\Gamma$ denotes the submatrix whose rows comprise the rows of $\mathbf{\Phi}$ that are defined in Γ. The expectation operator is given by $E\{\cdot\}$. $\mathrm{mod}\,(x,y) = x - \lfloor x/y \rfloor y$ if $y \neq 0$ and $x - \lfloor x/y \rfloor y \neq 0$, whereas $\mathrm{mod}\,(x,y) = y$ if $y \neq 0$ and $x - \lfloor x/y \rfloor y = 0$.

II. SYSTEM MODEL

We first introduce the proposed LS-SM-MIMO scheme and then focus our attention on the UL transmission with an emphasis on the multiuser signal detection.

A. Proposed Multiuser LS-SM-MIMO Scheme

As shown in Fig. 1, we consider the proposed LS-SM-MIMO from both the BS side and the user side. For conventional LS-MIMO, the number of AEs employed by the BS is equal to the number of its RF

chains [4]. However, the BS in LS-SM-MIMO, as shown in Fig. 1, is equipped with a much smaller number of RF chains M_{RF} than the total number of AEs M, i.e., we have $M_{\mathrm{RF}} \ll M$. Conventional LS-MIMO systems typically assume single-antenna users [4]. By contrast, in the proposed scheme, each user is equipped with $n_t > 1$ AEs but only a single RF chain, and SM is adopted for the UL transmission, where only one of the available AEs is activated for data transmission. It has been shown that the main power consumption and hardware cost of cellular networks comes from the radio access network [1]. Hence, using a reduced number of expensive RF chains compared with the total number of AEs at the BS can substantially reduce both the power consumption and the hardware cost for the operators. Meanwhile, it is feasible to incorporate several AEs and a single RF chain in the handsets. The resultant increased degrees of freedom in the spatial domain may then be exploited for improving the UL throughput. The proposed scheme can be considered as an optional UL-transmission mode in conventional LS-MIMO systems, where AE selection schemes may be adopted for beneficially selecting the most suitable M_{RF} AEs at the BS to receive UL SM signals [7]. Alternatively, it can also be used for the UL of LS-SM-MIMO, when advantageously combining transmit precoding, receive AE selection, and channel estimation [7]–[9].

B. Uplink Multiuser Transmission

We first consider the generation of SM signals at the users. The SM signal $\mathbf{x}_k = \mathbf{e}_k s_k$ transmitted by the kth user in a time slot consists of two parts: the spatial constellation symbol $\mathbf{e}_k \in \mathbb{C}^{n_t}$ and the signal constellation symbol $s_k \in \mathbb{C}$. $\mathbf{e}_k$ is generated by mapping $\lfloor \log_2(n_t) \rfloor$ bits to the index of the active AE, and typically, the user terminal employs $n_t = 2^p$ AEs, where p is a positive integer. Due to only a single RF chain employed at each user, only one entry of $\mathbf{e}_k$ associated with the active AE is equal to one, and the rest of the entries of $\mathbf{e}_k$ are zeros, i.e., we have

$$\mathrm{supp}(\mathbf{e}_k) \in \mathbb{A}, \quad \|\mathbf{e}_k\|_0 = 1, \quad \|\mathbf{e}_k\|_2 = 1 \qquad (1)$$

where $\mathbb{A} = \{1, 2, \ldots, n_t\}$ is the spatial constellation symbol set. The signal constellation symbol comes from L-ary modulation, i.e., $s_k \in \mathbb{L}$, where $\mathbb{L}$ is the signal constellation symbol set [e.g., 64 quadrature amplitude modulation (QAM)] of size L. Hence, each UL user's SM signal carries the information of $\log_2(L) + \log_2(n_t)$ bits per channel use (bpcu), and the overall UL throughput is $K(\log_2(L) + \log_2(n_t))$ bpcu. The users rely on the CPSC scheme for transmitting their SM signals [6]. Explicitly, each CPSC block consists of a cyclic prefix (CP) having the length of $P - 1$ and the associated data block having the length of Q. Hence, the length of each CPSC block is $Q + P - 1$, where this CP is capable of counteracting a dispersive multipath channel imposing dispersion over P samples. The concatenated data block consists of Q successive SM signals.

At the receiver, due to the reduced number of RF chains at the BS, only M_{RF} receive AEs can be exploited to receive signals, where existing receive AE selection schemes can be adopted to preselect M_{RF} receive AEs for achieving an improved signal detection performance [7]. Since the BS can serve K users simultaneously, after the removal of the CP, the received signal $\mathbf{y}_q \in \mathbb{C}^{M_{\mathrm{RF}}}$ for $1 \leq q \leq Q$ of the qth time slot of a specific CPSC block can be expressed as

$$\mathbf{y}_q = \sum_{k=1}^{K} \mathbf{y}_{k,q} + \mathbf{w}_q = \sum_{p=0}^{P-1} \sum_{k=1}^{K} \mathbf{H}_{k,p}\rangle_\Theta \mathbf{x}_{k,\ \mathrm{mod}\,(q-p,Q)} + \mathbf{w}_q$$

$$= \sum_{p=0}^{P-1} \sum_{k=1}^{K} \tilde{\mathbf{H}}_{k,p} \mathbf{x}_{k,\ \mathrm{mod}\,(q-p,Q)} + \mathbf{w}_q \qquad (2)$$

where $\mathbf{H}_{k,p} \in \mathbb{C}^{M \times n_t}$ is the kth user's MIMO channel matrix for the pth multipath component, i.e., $\mathbf{H}_{k,p}\rangle_\Theta = \tilde{\mathbf{H}}_{k,p} \in \mathbb{C}^{M_{\mathrm{RF}} \times n_t}$; the set Θ is determined by the AE selection scheme used; the elements of Θ having the cardinality of M_{RF} are uniquely selected from the set $\{1, 2, \ldots, M\}$; $\mathbf{x}_{k,q}$ has one nonzero entry; and $\mathbf{w}_q \in \mathbb{C}^{M_{\mathrm{RF}}}$ is the additive white Gaussian noise (AWGN) vector with entries obeying the independent and identically distributed (i.i.d.) circularly symmetric complex Gaussian distribution with zero mean and a variance of $\sigma_w^2/2$ per dimension, which is denoted by $\mathcal{CN}(0, \sigma_w^2)$. $\mathbf{H}_{k,p} = \mathbf{R}_{\mathrm{BS}}^{1/2} \bar{\mathbf{H}}_{k,p} \mathbf{R}_{\mathrm{US}}^{1/2}$, the entries of $\bar{\mathbf{H}}_{k,p}$ obey the i.i.d. $\mathcal{CN}(0, 1)$, and $\mathbf{R}_{\mathrm{US}}$ with the correlation coefficient ρ_{US} and $\mathbf{R}_{\mathrm{BS}}$ with the correlation coefficient ρ_{BS} are correlation matrices at the users and the BS, respectively. The specific element of the mth row and the nth column of R_{BS} (R_{US}) is $\rho_{\mathrm{BS}}^{|m-n|}$ ($\rho_{\mathrm{US}}^{|m-n|}$). For correlated Rayleigh-fading MIMO channels, the specific Θ or receive AE selection scheme has an impact on the attainable system performance. In this paper, the direct AE selection scheme is used for maximizing the minimum geometric distance between any pair of the selected AEs [7]. For uniform linear arrays (ULAs), $\Theta = \{\varphi + m_{\mathrm{RF}}\lfloor M/M_{\mathrm{RF}} \rfloor\}_{m_{\mathrm{RF}}=0}^{M_{\mathrm{RF}}-1}$ with $1 \leq \varphi \leq \lfloor M/M_{\mathrm{RF}} \rfloor - 1$. Then, (2) can be further expressed as

$$\mathbf{y}_q = \sum_{p=0}^{P-1} \tilde{\mathbf{H}}_p \mathbf{x}_{\bmod(q-p,Q)} + \mathbf{w}_q \qquad (3)$$

by defining $\tilde{\mathbf{H}}_p = [\tilde{\mathbf{H}}_{1,p} \tilde{\mathbf{H}}_{2,p}, \ldots, \tilde{\mathbf{H}}_{K,p}] \in \mathbb{C}^{M_{\mathrm{RF}} \times (n_t K)}$ and $\mathbf{x}_q = [(\mathbf{x}_{1,q})^T (\mathbf{x}_{2,q})^T, \ldots, (\mathbf{x}_{K,q})^T]^T \in \mathbb{C}^{(n_t K)}$. By considering the Q SM signals of a specific CPSC block, we arrive at

$$\mathbf{y} = \tilde{\mathbf{H}}\mathbf{x} + \mathbf{w} \qquad (4)$$

where $\mathbf{y} = [(\mathbf{y}_1)^T (\mathbf{y}_2)^T, \ldots, (\mathbf{y}_Q)^T]^T \in {}^{(M_{\mathrm{RF}}Q)}$, the aggregate SM signal $\mathbf{x} = [(\mathbf{x}_1)^T (\mathbf{x}_2)^T, \ldots, (\mathbf{x}_Q)^T]^T \in {}^{(Kn_tQ)}$, $\mathbf{w} = [(\mathbf{w}_1)^T (\mathbf{w}_2)^T, \ldots, (\mathbf{w}_Q)^T]^T$, and

$$\tilde{\mathbf{H}} = \begin{bmatrix} \tilde{\mathbf{H}}_0 & \mathbf{0} & \mathbf{0} & \cdots & \tilde{\mathbf{H}}_2 & \tilde{\mathbf{H}}_1 \\ \tilde{\mathbf{H}}_1 & \tilde{\mathbf{H}}_0 & \mathbf{0} & \cdots & \vdots & \tilde{\mathbf{H}}_2 \\ \vdots & \tilde{\mathbf{H}}_1 & \tilde{\mathbf{H}}_0 & \cdots & \tilde{\mathbf{H}}_{P-1} & \vdots \\ \tilde{\mathbf{H}}_{P-1} & \vdots & \tilde{\mathbf{H}}_1 & \cdots & \mathbf{0} & \tilde{\mathbf{H}}_{P-1} \\ \mathbf{0} & \tilde{\mathbf{H}}_{P-1} & \vdots & \vdots & \vdots & \mathbf{0} \\ \vdots & \mathbf{0} & \tilde{\mathbf{H}}_{P-1} & \vdots & \vdots & \vdots \\ \vdots & \vdots & \mathbf{0} & \vdots & \mathbf{0} & \vdots \\ \vdots & \vdots & \vdots & \vdots & \tilde{\mathbf{H}}_0 & \mathbf{0} \\ \mathbf{0} & \mathbf{0} & \mathbf{0} & \cdots & \tilde{\mathbf{H}}_1 & \tilde{\mathbf{H}}_0 \end{bmatrix}. \qquad (5)$$

The signal-to-noise ratio (SNR) at the receiver is defined by SNR $= E\{\|\tilde{\mathbf{H}}\mathbf{x}\|_2^2\}/E\{\|\mathbf{w}\|_2^2\}$.

The optimal signal detector for (4) relies on the ML algorithm, i.e.,

$$\min_{\hat{\mathbf{x}}} \quad \|\mathbf{y} - \tilde{\mathbf{H}}\hat{\mathbf{x}}\|_2 = \min_{\{\hat{\mathbf{x}}_{k,q}\}_{k=1, q=1}^{K, Q}} \|\mathbf{y} - \tilde{\mathbf{H}}\hat{\mathbf{x}}\|_2$$

$$\text{s.t.} \quad \mathrm{supp}(\hat{\mathbf{x}}_{k,q}) \in \mathbb{A}, \hat{\mathbf{x}}_{k,q}\rangle_{\mathrm{supp}(\hat{\mathbf{x}}_{k,q})} \in \mathbb{L}, \ 1 \leq k \leq K, 1 \leq q \leq Q \qquad (6)$$

whose complexity exponentially increases with the number of users, since the size of the search set for the ML detector is $(n_t \cdot L)^{KQ}$. This excessive complexity can be unaffordable in practice. To reduce the complexity, near-optimal sphere decoding detectors have been proposed [10], but their complexity may still remain high, particularly

for the systems supporting large K, Q, n_t, and L [11]. In conventional LS-MIMO systems, low-complexity linear signal detectors (e.g., the MMSE-based signal detector) have been shown to be near optimal since $M = M_{\mathrm{RF}} \gg K$ and $n_t = 1$ make multiuser signal detection an *overdetermined* problem [4]. However, in the proposed scheme, we have $M_{\mathrm{RF}} < Kn_t$. Hence, the multiuser signal detection problem (6) represents a large-scale *underdetermined* problem. Consequently, the conventional linear signal detectors perform poorly in the proposed LS-SM-MIMO [11]. By exploiting the sparsity of SM signals, the authors in [11]–[13] have proposed the concept of CS-based signal detectors for the downlink of small-scale SM-MIMO operating in a single-user scenario. However, these signal detectors are unsuitable for the proposed multiuser scenarios. Observe from (1) that $\mathbf{x}_{k,q}$ is a sparse signal having a sparsity level of one. Hence, the aggregate SM signal $\mathbf{x}$, which consists of multiple users' SM signals in Q time slots, exhibits distributed sparsity with the sparsity level of KQ. This property of $\mathbf{x}$ inspires us to exploit the SCS theory for the multiuser signal detection [14]. To further improve the signal detection performance and to increase the system's throughput, we propose a joint SM transmission scheme and an SCS-based MUD, which will be detailed in the following section.

III. SCS-Based MUD for LS-SM-MIMO UL

To solve the multiuser signal detection of our UL LS-SM-MIMO system, we first propose a joint SM transmission scheme to be employed at the users. Accordingly, an SCS-based low-complexity MUD is developed at the BS, whereby the distributed sparsity of the aggregate SM signal and the group sparsity of multiple aggregate SM signals are exploited. Moreover, the computational complexity of the proposed SCS-based MUD is discussed.

A. Joint SM Transmission Scheme at the Users

For the kth user in the qth time slot, every successive J CPSC block is considered as a group, and they share the same spatial constellation symbol, i.e.,

$$\mathrm{supp}\left(\mathbf{x}_{k,q}^{(1)}\right) = \mathrm{supp}\left(\mathbf{x}_{k,q}^{(2)}\right) = \cdots = \mathrm{supp}\left(\mathbf{x}_{k,q}^{(J)}\right),$$
$$1 \leq k \leq K, 1 \leq q \leq Q \qquad (7)$$

where we introduce the superscript (j) to denote the jth CPSC block, and J is typically small, e.g., $J = 2$. In CS theory, the specific signal structure, where $\mathbf{x}_{k,q}^{(1)}, \mathbf{x}_{k,q}^{(2)}, \ldots, \mathbf{x}_{k,q}^{(J)}$ share a common support, is often referred to as the *group sparsity*. Similarly, the aggregate SM signals consisting of the K users' SM signals also exhibit group sparsity, i.e.,

$$\mathrm{supp}(\mathbf{x}^{(1)}) = \mathrm{supp}(\mathbf{x}^{(2)}) = \cdots = \mathrm{supp}(\mathbf{x}^{(J)}). \qquad (8)$$

Although exhibiting group sparsity may slightly reduce the information carried by the spatial constellation symbols, it is also capable of reducing the number of the RF chains required according to the SCS theory, while simultaneously improving the total bit error rate (BER) of the entire system even with higher UL throughput. This conclusion will be confirmed by our simulation results.

B. SCS-Based MUD at the BS

According to (4), the received signals at the BS in the same group can be expressed as

$$\mathbf{y}^{(j)} = \tilde{\mathbf{H}}^{(j)}\mathbf{x}^{(j)} + \mathbf{w}^{(j)}, \quad 1 \leq j \leq J \qquad (9)$$

where $\mathbf{y}^{(j)}$ denotes the received signal in the jth CPSC block, whereas $\tilde{\mathbf{H}}^{(j)}$ and $\mathbf{w}^{(j)}$ are the effective MIMO channel matrix and the AWGN vector, respectively.

The intrinsically distributed sparsity of $\mathbf{x}^{(j)}$ and the underdetermined nature of (9) inspire us to solve the signal detection problem based on CS theory, which can efficiently acquire the sparse solutions to underdetermined linear systems. Moreover, the J different aggregate SM signals in (9) can be jointly exploited for improving the signal detection performance due to the group sparsity of $\{\mathbf{x}^{(j)}\}_{j=1}^{J}$. Thus, by considering both the distributed sparsity and the group sparsity of the aggregate SM signals, the multiuser signal detection at the BS can be formulated as the following optimization problem:

$$\min_{\{\widehat{\mathbf{x}}^{(j)}\}_{j=1}^{J}} \quad \sum_{j=1}^{J} \left\| \mathbf{y}^{(j)} - \tilde{\mathbf{H}}^{(j)}\widehat{\mathbf{x}}^{(j)} \right\|_2^2$$

$$= \min_{\{\widehat{\mathbf{x}}_{k,q}^{(j)}\}_{j=1,k=1,q=1}^{J,K,Q}} \sum_{j=1}^{J} \left\| \mathbf{y}^{(j)} - \tilde{\mathbf{H}}^{(j)}\widehat{\mathbf{x}}^{(j)} \right\|_2^2$$

$$\text{s.t.} \quad \left\| \widehat{\mathbf{x}}_{k,q}^{(j)} \right\|_0 = 1, \ 1 \le j \le J, \ 1 \le q \le Q, \ 1 \le k \le K. \tag{10}$$

Our proposed SCS-based MUD solves the optimization problem (10) with the aid of two steps. In the first step, we estimate the spatial constellation symbols, i.e., the indexes of K users' active AEs in J successive CPSC blocks. In the second step, we infer the legitimate signal constellation symbols of the K users in J CPSC blocks.

1. Step 1— Estimation of Spatial Constellation Symbols: We propose a group subspace pursuit (GSP) algorithm developed from the classical subspace pursuit (SP) algorithm in [15] to acquire the sparse solution to the large-scale underdetermined problem (10), where both the *a priori* sparse information (i.e., $\|\mathbf{x}_{k,q}^{(j)}\|_0 = 1$) and the group sparsity of $\mathbf{x}^{(1)}, \mathbf{x}^{(2)}, \ldots, \mathbf{x}^{(J)}$ are exploited for improving the multiuser signal detection performance. The proposed GSP algorithm is described in **Algorithm 1**, which estimates SM signal $\{\widehat{\mathbf{x}}_{k,q}^{(j)}\}_{k=1,j=1,q=1}^{K,J,Q}$. Hence, the estimated spatial constellation symbol is $\{\text{supp}(\widehat{\mathbf{x}}_{k,q}^{(j)})\}_{k=1,j=1,q=1}^{K,J,Q}$.

Algorithm 1 Proposed GSP Algorithm.

Input: Noisy received signals $\mathbf{y}^{(j)}$ and effective channel matrices $\tilde{\mathbf{H}}^{(j)}$ for $1 \le j \le J$.

Output: Estimated $\widehat{\mathbf{x}}^{(j)} = [(\widehat{\mathbf{x}}_1^{(j)})^T (\widehat{\mathbf{x}}_2^{(j)})^T, \ldots, (\widehat{\mathbf{x}}_Q^{(j)})^T]^T$, where $\widehat{\mathbf{x}}_q^{(j)} = [(\widehat{\mathbf{x}}_{1,q}^{(j)})^T (\widehat{\mathbf{x}}_{2,q}^{(j)})^T, \ldots, (\widehat{\mathbf{x}}_{K,q}^{(j)})^T]^T$ for $1 \le q \le Q$.

1: $\mathbf{r}^{(j)} = \mathbf{y}^{(j)}$ for $1 \le j \le J$; {Initialization}
2: $\Omega^0 = \emptyset$; {Empty support set}
3: $t = 1$; {Iteration index}
4: **repeat**
5: $\quad \mathbf{a}_{k,q}^{(j)} = (\tilde{\mathbf{H}}_{k,q}^{(j)})^{*} \mathbf{r}^{(j)}$ for $1 \le k \le K$, $1 \le q \le Q$, and $1 \le j \le J$; {Correlation}
6: $\quad \tau_{k,q} = \arg\max_{\widetilde{\tau}_{k,q}} \sum_{j=1}^{J} \|\mathbf{a}_{k,q}^{(j)}\rangle_{\widetilde{\tau}_{k,q}} t\|_2^2$ for $1 \le k \le K$, $1 \le q \le Q$; {Identify support}
7: $\quad \Gamma = \{\tau_{k,q} + (k-1+K(q-1))n_t\}_{k=1,q=1}^{K,Q}$; {Preliminary support set}
8: $\quad \mathbf{b}^{(j)}|_{\Omega^{t-1}\cup\Gamma} = (\tilde{\mathbf{H}}^{(j)}|_{\Omega^{t-1}\cup\Gamma})^{\dagger}\mathbf{y}^{(j)}$ for $1 \le j \le J$; {Least squares}
9: $\quad \omega_{k,q} = \arg\max_{\widetilde{\omega}_{k,q}} \sum_{j=1}^{J} \|\mathbf{b}_{k,q}^{(j)}\rangle_{\widetilde{\omega}_{k,q}}\|_2^2$ for $1 \le k \le K$, $1 \le q \le Q$; {Pruning support set}
10: $\quad \Omega^t = \{\omega_{k,q} + (k-1+K(q-1))n_t\}_{k=1,q=1}^{K,Q}$; {Final support set}
11: $\quad \mathbf{c}^{(j)}|_{\Omega^t} = (\tilde{\mathbf{H}}^{(j)}|_{\Omega^t})^{\dagger}\mathbf{y}^{(j)}$ for $1 \le j \le J$; {Least squares}
12: $\quad \mathbf{r}^{(j)} = \mathbf{y}^{(j)} - \tilde{\mathbf{H}}^{(j)}\mathbf{c}^{(j)}$ for $1 \le j \le J$; {Compute residual}
13: $\quad t = t + 1$; {Update iteration index}
14: **until** $\Omega^t = \Omega^{t-1}$ or $t \ge Q$

Compared with the classical SP algorithm, the proposed GSP algorithm exploits the distributed sparsity and group sparsity of $\{\mathbf{x}^{(j)}\}_{j=1}^{J}$. More explicitly, $\mathbf{x}^{(j)} \in \mathbb{C}^{(KQn_t)}$ consists of the KQ low-dimensional sparse vectors $\mathbf{x}_{k,q}^{(j)} \in \mathbb{C}^{n_t}$, where each $\mathbf{x}_{k,q}^{(j)}$ has the known sparsity level of one, and the aggregate SM signals $\mathbf{x}^{(1)}, \mathbf{x}^{(2)}, \ldots, \mathbf{x}^{(J)}$ exhibit group sparsity. Specifically, the differences between the proposed GSP algorithm and the classical SP algorithm lie in the following two aspects: 1) the identification of the support set including the steps of the *preliminary support set* and the *final support set* as shown in **Algorithm 1**; and 2) the joint processing of $\mathbf{y}^{(1)}, \mathbf{y}^{(2)}, \ldots, \mathbf{y}^{(J)}$. First, for the support selection, taking the step of the *preliminary support set* for instance, when selecting the preliminary support set, the classical SP algorithm selects the support set associated with the first KQ largest values of the global correlation result $(\tilde{\mathbf{H}}^{(j)})^{*}\mathbf{r}^{(j)}$. By contrast, the proposed GSP algorithm selects the support set associated with the largest value from the local correlation result in each $(\tilde{\mathbf{H}}_{k,q}^{(j)})^{*}\mathbf{r}^{(j)}$. This way, the distributed sparsity of the aggregate SM signal can be exploited for improved signal detection performance. Second, compared with the classical SP algorithm, the proposed GSP algorithm jointly exploits the J correlated signals having the group sparsity, which can bring the further improved signal detection performance.

It should be noted that even for the special case of $J = 1$, i.e., without using the joint SM transmission scheme, the proposed GSP algorithm still achieves a better signal detection performance than the classical SP algorithm when handling the aggregate SM signal, since the inherently distributed sparsity of the aggregate SM signal is leveraged to improve the signal detection performance.

2. Step 2— Acquisition of Signal Constellation Symbols: Following *Step 1*, we can also acquire a rough estimate of the signal constellation symbol for each user in each time slot. By searching for the minimum Euclidean distance between this rough estimate of the signal constellation symbol and the legitimate constellation symbols of $\mathbb{L}$, we can obtain the final estimate of signal constellation symbols.

C. Computational Complexity

The optimal ML signal detector has a prohibitively high computational complexity of $\mathcal{O}((L \cdot n_t)^{(K \cdot Q)})$ according to (6). The sphere decoding detectors [10] are indeed capable of reducing the computational complexity, but they may still suffer from unaffordable complexity, particularly for large K, Q, L, and n_t values. By contrast, the conventional MMSE-based detector for LS-MIMO and CS-based detector [13] for small-scale SM-MIMO enjoy the low complexity of $\mathcal{O}(M_{\text{RF}} \cdot (n_t \cdot Q \cdot K)^2 + (n_t \cdot Q \cdot K)^3)$ and $\mathcal{O}(2M_{\text{RF}} \cdot (Q \cdot K)^2 + (Q \cdot K)^3)$, respectively. For the proposed SCS-based MUD, most of the computational requirements are imposed by the least squares (LS) operations, which has complexity of $\mathcal{O}(J \cdot (2M_{\text{RF}} \cdot (Q \cdot K)^2 + (Q \cdot K)^3))$ [16]. Consequently, the computational complexity per CPSC block is $\mathcal{O}(2M_{\text{RF}} \cdot (Q \cdot K)^2 + (Q \cdot K)^3)$, since J successive aggregate SM signals are jointly processed. Compared with conventional signal detectors, the proposed SCS-based MUD benefits from substantially lower complexity, and it has similar low complexity as the conventional MMSE- and CS-based signal detectors.
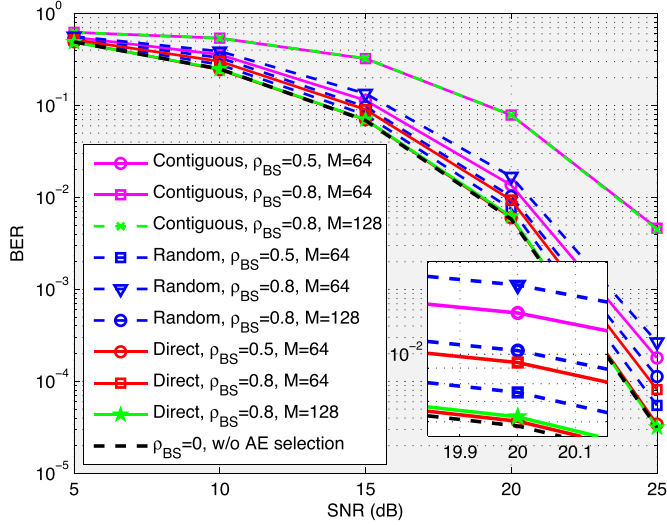
Fig. 2. Total BERs achieved by the proposed SCS-based MUD with different AE selection schemes, where $K = 8$, $J = 2$, 64-QAM, $M_{RF} = 18$, $n_t = 4$, and $\rho_{US} = 0$ are considered.

Fig. 3. Total BERs achieved by the CS-based signal detector and the SCS-based MUD against different SNRs in LS-SM-MIMO, where $K = 8$, $M_{RF} = 18$, $M = 64$, $\rho_{BS} = 0.5$, and the direct AE selection scheme is considered.

IV. SIMULATION RESULTS

A simulation study was carried out to compare the attainable performance of the proposed SCS-based MUD to that of the MMSE-based signal detector [4] and to that of the CS-based signal detector [13]. In the LS-SM-MIMO system considered, the BS used a ULA relying on a large number of AEs M, but a much smaller number of RF chains M_{RF}, whereas K users employing n_t AEs but only a single RF chain simultaneously use the CPSC scheme associated with $P = 8$ and $Q = 64$ to transmit the SM signals to the BS. The total BER including both the spatial constellation symbols and the signal constellation symbols was evaluated.

Fig. 2 compares the total BERs achieved by the proposed SCS-based MUD with different AE selection schemes, where $K = 8$, $J = 2$, 64-QAM, $M_{RF} = 18$, $n_t = 4$, and $\rho_{US} = 0$ are considered. The contiguous AE selection scheme implies that we select M_{RF} adjacent AEs, i.e., $\Theta = \{\varphi + m_{RF}\}_{m_{RF}=0}^{M_{RF}-1}$ with $1 \leq \varphi \leq M - M_{RF} + 1$. By contrast, in the random AE selection scheme, the elements of Θ are randomly selected from the set $\{1, 2, \ldots, M\}$, whereas the direct AE selection scheme in [7] has been described in Section II-B. Furthermore, the BER achieved by the SCS-based MUD relying on $\rho_{BS} = 0$ is also considered as a performance bound, since the choice of $\rho_{BS} = 0$ and $\rho_{US} = 0$ implies the uncorrelated Rayleigh-fading MIMO channels. Observe from Fig. 2 that the direct AE selection scheme outperforms the other pair of AE selection schemes. Moreover, for a certain AE selection scheme, the BER performance degrades when M_{RF}/M or ρ_{BS} increases. For the direct AE selection scheme, the BER performance of $\rho_{BS} = 0.8$, $M = 128$ and of $\rho_{BS} = 0.5$, $M = 64$ approaches the BER achieved for transmission over uncorrelated Rayleigh-fading MIMO channels, which confirms the near-optimal performance of the direct AE selection scheme.

Fig. 3 compares the overall BER achieved by the CS-based signal detector and by the proposed SCS-based MUD versus the SNR in our LS-SM-MIMO context, where $K = 8$, $M_{RF} = 18$, $M = 64$, $\rho_{BS} = 0.5$, and the direct AE selection scheme is considered. The SCS-based MUD outperforms the CS-based signal detector even for $J = 1$, since the distributed sparsity of the aggregate SM signal is exploited. For the SCS-based MUD, the BER performance improves when J increases, albeit this is achieved at the cost of reduced UL throughput. To mitigate this impediment, a higher number of AEs can be employed by the users
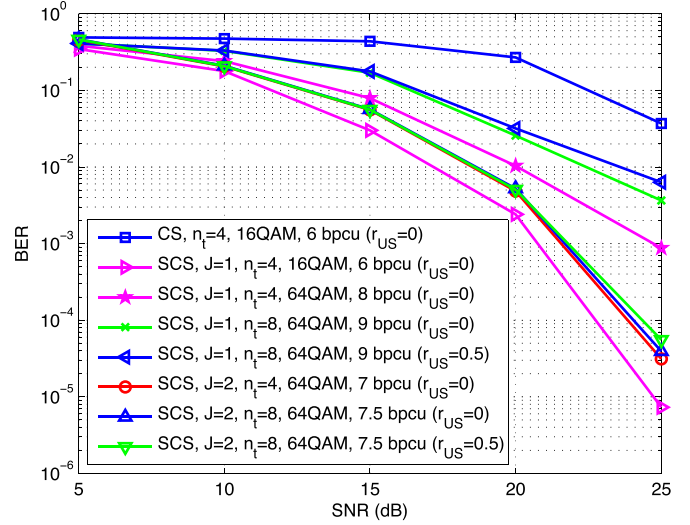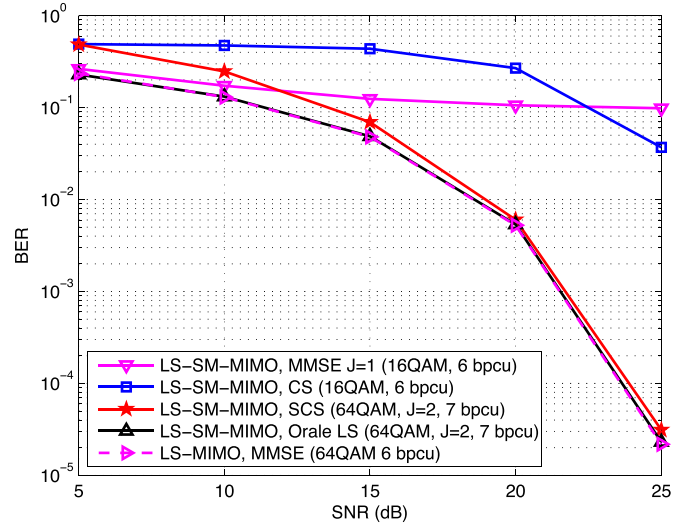

Fig. 4. Total BERs achieved by different signal detectors against different SNRs in the proposed LS-SM-MIMO and conventional LS-MIMO.

for expanding the spatial constellation symbol set constituted by the AEs. Specifically, by increasing n_t from 4 to 8, the UL throughput of the SCS-based MUD may be increased, but having more AEs at the user results in a higher ρ_{US}. When n_t is increased, the BER performance of the SCS-based MUD associated with $J = 1$ degrades, as expected. By contrast, when n_t is increased, the BER performance loss of the SCS-based MUD using $J = 2$ can be less than 0.2 dB if the BER of 10^{-4} is considered, even when a higher ρ_{US} associated with a higher n_t is considered.

Fig. 4 portrays the BER achieved by the different signal detectors as a function of the SNR in the context of the proposed LS-SM-MIMO for $K = 8$, $M_{RF} = 18$, $M = 64$, $n_t = 4$, $\rho_{BS} = 0.5$, and $\rho_{US} = 0$, where the direct AE selection scheme is also considered. In Fig. 4, we also characterize the 'oracle-assisted' LS-based signal detector relying on the assumption that the spatial constellation symbol is perfectly known at the BS for the proposed LS-SM-MIMO scheme associated with $J = 2$, 64-QAM as well as for the MMSE-based

LS-MIMO detector in conjunction with 64-QAM, where both of them only consider the BER of the classic signal constellation symbol. Here, we assume that the LS-MIMO arrangement uses the same number of RF chains to serve eight single-antenna users communicating over uncorrelated Rayleigh-fading channels. The superiority of our SCS-based MUD over the MMSE- and CS-based signal detectors becomes clear.

Moreover, the performance gap between the oracle LS-based signal detector associated with 7 bpcu and the proposed SCS-based MUD with 7 bpcu is less than 0.5 dB. Note again that the oracle LS-based signal detector only considers the BER of the classic signal constellation symbol, whereas the proposed SCS-based MUD considers both the spatial and the classic signal constellation symbols. Finally, compared with the conventional LS-MIMO using the MMSE-based signal detector (6 bpcu), our proposed UL LS-SM-MIMO and the associated SCS-based MUD (7 bpcu) only suffer from a negligible BER loss, which explicitly confirmed the improved UL throughput of the proposed LS-SM-MIMO scheme.

V. CONCLUSION

We have proposed an LS-SM-MIMO scheme for the UL transmission. The BS employs a large number of AEs but a much smaller number of RF chains, where a simple receive AE selection scheme is used for the improved performance. Each user equipped with multiple AEs but only a single RF chain uses CPSC to combat multipath channels. SM has been adopted for the UL transmission to improve the UL throughput. The proposed scheme is particularly suitable for scenarios where a large number of low-cost AEs can be accommodated, and both power consumption and hardware cost are heavily determined by the number of RF chains. Due to the reduced number of RF chains at the BS and multiple AEs employed by each user, the UL multiuser signal detection is a challenging large-scale underdetermined problem. We have proposed a joint SM transmission scheme at the users to introduce the group sparsity of multiple aggregate SM signals, and a matching SCS-based MUD at the BS has been proposed to leverage the inherently distributed sparsity of the aggregate SM signal as well as the group sparsity of multiple aggregate SM signals for reliable multiuser signal detection performance. The proposed SCS-based MUD enjoys the low complexity, and our simulation results have demonstrated that it performs better than its conventional counterparts with even much higher UL throughput.

REFERENCES

[1] M. D. Renzo, H. Haas, A. Ghrayeb, S. Sugiura, and L. Hanzo, "Spatial modulation for generalized MIMO: Challenges, opportunities and implementation," *Proc. IEEE*, vol. 102, no. 1, pp. 56–103, Jan. 2014.

[2] A. Younis, R. Mesleh, M. Di Renzo, and H. Haas, "Generalised spatial modulation for large-scale MIMO," in *Proc. EUSIPCO*, Sep. 2014, pp. 346–350.

[3] S. Ganesan, R. Mesleh, H. Haas, C. Ahn, and S. Yun, "On the performance of spatial modulation OFDM," in *Proc. 40th Asilomar Conf. Signals, Syst. Comput.*, Oct. 2006, pp. 1825–1829.

[4] F. Rusek *et al.* "Scaling up MIMO: Opportunities and challenges with very large arrays," *IEEE Signal Process. Mag.*, vol. 30, no. 1, pp. 40–60, Jan. 2013.

[5] N. Serafimovski *et al.*, "Practical implementation of spatial modulation," *IEEE Trans. Veh. Technol.*, vol. 62, no. 9, pp. 4511–4523, Nov. 2013.

[6] P. Som and A. Chockalingam, "Spatial modulation and space shift keying in single carrier" in *Proc. IEEE Int. Symp. PIMRC*, Sep. 2012, pp. 1062–1067.

[7] X. Wu, M. Di Renzo, and H. Haas, "Adaptive selection of antennas for optimum transmission in spatial modulation," *IEEE Trans. Wireless Commun.*, vol. 14, no. 7, pp. 3630–3641, Jul. 2015.

[8] S. Narayanan *et al.*, "Multi-user spatial modulation MIMO" in *Proc. IEEE WCNC*, Apr. 2014, pp. 671–676.

[9] X. Wu, H. Claussen, M. D. Renzo, and H. Haas, "Channel estimation for spatial modulation," *IEEE Trans. Commun.*, vol. 62, no. 12, pp. 4362–4372, Dec. 2014.

[10] A. Younis, S. Sinanovic, M. Di Renzo, R. Mesleh, and H. Haas, "Generalised sphere decoding for spatial modulation," *IEEE Trans. Commun.*, vol. 61, no. 7, pp. 2805–2815, Jul. 2013.

[11] W. Liu, N. Wang, M. Jin, and H. Xu, "Denoising detection for the generalized spatial modulation system using sparse property," *IEEE Commun. Lett.*, vol. 18, no. 1, pp. 22–25, Jan. 2014.

[12] B. Shim, S. Kwon, and B. Song, "Sparse detection with integer constraint using multipath matching pursuit," *IEEE Commun. Lett.*, vol. 18, no. 10, pp. 1851–1854, Oct. 2014.

[13] C. Yu *et al.*, "Compressed sensing detector design for space shift keying in MIMO systems," *IEEE Commun. Lett.*, vol. 16, no. 10, pp. 1556–1559, Oct. 2012.

[14] M. F. Duarte and Y. C. Eldar, "Structured compressed sensing: From theory to applications," *IEEE Trans. Signal Process.*, vol. 59, no. 9, pp. 4053–4085, Sep. 2011.

[15] W. Dai and O. Milenkovic, "Subspace pursuit for compressive sensing signal reconstruction," *IEEE Trans. Inf. Theory*, vol. 55, no. 5, pp. 2230–2249, May 2009.

[16] A. Björck, *Numerical Methods for Matrix Computations*. Cham, Switzerland: Springer Int. Publ. AG, 2014.

Receiver Architecture for Frequency Offset Correction and I/Q Imbalance Compensation in Equal Bandwidth Contiguous Carrier Aggregation

Ahmad Gomaa and Louay M. A. Jalloul, *Senior Member, IEEE*

Abstract—A highly efficient receiver architecture for intraband contiguous carrier aggregation (CA) is described. The downconversion architecture is done in two stages; the first stage is done in the analog domain using a direct-conversion receiver, whereas the second stage is done in the digital domain using offset frequency digital mixing to separate the carriers. The novelty in the architecture stems from its ability to compensate for the different carrier frequency offsets (CFOs) between the two transmitted carriers, and unlike traditional approaches, the receiver uses a *single* complex digital mixer for baseband carrier separation. The receiver architecture also compensates for in-phase and quadrature gain and phase imbalance (IQI) inherent in direct-conversion receivers. It is shown that, in our new architecture, IQI compensation can be done *post* the digital mixer, thus enabling a low-power implementation to this impairment.

Index Terms—Carrier aggregation, frequency offset correction, in-phase and quadrature (I/Q) imbalance, radio-frequency (RF) impairments, single RF receiver.

I. INTRODUCTION

Carrier aggregation (CA) is a technique used to increase the data rate between the transmitter and the receiver. This aggregation is achieved by the concatenation of two or more component carriers (CCs) [1],